



UNIVERSITY OF LEEDS

This is a repository copy of *Field-induced refractive index variation in the dark conglomerate phase for polarization-independent switchable liquid crystal lenses.*

White Rose Research Online URL for this paper:
<http://eprints.whiterose.ac.uk/86441/>

Version: Accepted Version

Article:

Milton, HE, Nagaraj, M, Kaur, S et al. (3 more authors) (2014) Field-induced refractive index variation in the dark conglomerate phase for polarization-independent switchable liquid crystal lenses. *Applied Optics*, 53 (31). 7278 - 7232. ISSN 1559-128X

<https://doi.org/10.1364/AO.53.007278>

Reuse

Unless indicated otherwise, fulltext items are protected by copyright with all rights reserved. The copyright exception in section 29 of the Copyright, Designs and Patents Act 1988 allows the making of a single copy solely for the purpose of non-commercial research or private study within the limits of fair dealing. The publisher or other rights-holder may allow further reproduction and re-use of this version - refer to the White Rose Research Online record for this item. Where records identify the publisher as the copyright holder, users can verify any specific terms of use on the publisher's website.

Takedown

If you consider content in White Rose Research Online to be in breach of UK law, please notify us by emailing eprints@whiterose.ac.uk including the URL of the record and the reason for the withdrawal request.



eprints@whiterose.ac.uk
<https://eprints.whiterose.ac.uk/>

Field-induced refractive index variation in the dark conglomerate phase for polarization-independent switchable liquid crystal lenses

H. E. Milton^{1,2}, M. Nagaraj¹, S. Kaur^{1,2}, J. C. Jones¹, P. B. Morgan² and H. F. Gleeson^{1*}

¹*School of Physics and Astronomy, University of Manchester, Manchester, M13 9PL, United Kingdom*

²*Eurolens Research, Faculty of Life Sciences, University of Manchester, Manchester, M13 9PL, United Kingdom*

*Corresponding author: helen.gleeson@manchester.ac.uk

Received Month X, XXXX; revised Month X, XXXX; accepted Month X, XXXX;
 posted Month X, XXXX (Doc. ID XXXXX); published Month X, XXXX

Liquid crystal lenses are an emerging technology that can provide variable focal power in response to an applied voltage. Many designs for liquid crystal based lenses are polarization dependent, so that 50% of light is not focused as required, making polarization-independent technologies very attractive. Recently, the dark conglomerate phase, which is an optically isotropic liquid crystalline state, has been shown to exhibit a large change in refractive index in response to an applied electric field ($\Delta n = 0.04$). This paper describes computational modelling of the electrostatic solutions for two different types of 100 μm diameter liquid crystal lenses that include the dark conglomerate phase, demonstrating that it shows great potential for efficient isotropic optical switching in lenses. A feature of the field dependence of the refractive index change in the dark conglomerate phase is that it is approximately linear in a certain range, leading to the prediction of excellent optical quality for driving fields in this regime. Interestingly, a simulated microlens is shown to exhibit two modes of operation, a positive lens based upon a uniform bulk change in refractive index at high voltages, and a negative lens resulting from the induction of a gradient index effect at intermediate voltages.

© 2014 Optical Society of America

OCIS codes: (170.0110) Imaging systems; (170.3010) Image reconstruction techniques; (170.3660) Light propagation in tissues.

<http://dx.doi.org/10.1364/AO.99.099999>

1. Introduction

Liquid crystal lenses have shown great potential for a wide range of applications, with the ability to change between focal states making them excellent candidates for a growing number of switchable devices [1]. Liquid crystal lenses operate *via* a change in the material refractive index, which occurs in response to an applied voltage. The most commonly used liquid crystals are in the nematic phase in which anisotropic rod-like molecules tend to align in a preferred direction known as the director. The director is often initially aligned parallel to the surface of the device (planar alignment) and the maximum voltage induced change in refractive index then corresponds to a transition between the extraordinary and ordinary indices, n_e and n_o .

There are several different methods of producing a variable lens using nematic liquid crystals, with the three main techniques including the use of a lens-shaped liquid crystal layer [2-4], a flat gradient index (GRIN) lens profile arising from a parabolic electric field [5-7] and using a diffractive optical structure [8]. However, an issue with many nematic liquid crystal lens designs is that they are polarization dependent, with only 50% of unpolarized light, the proportion polarized parallel to the director, being subject to the variable change in focal power. Approaches that have been suggested to overcome the

polarization dependence in nematic-based lenses include the use of a twisted nematic geometry [9] or including multiple liquid crystal layers in the lens design [10]. Blue phase liquid crystals have also been suggested as an optically isotropic solution [11]. However, there are disadvantages associated with each of these approaches: the solutions that employ nematic liquid crystals are more complex in device construction, while the switching mode used in blue phases is the Kerr effect, which suffers from inherent chromatic aberration associated with the wavelength dependence of the Kerr constant and often requires high voltages to induce a sufficiently large birefringence.

The emergence of new electro-optic switching modes that occur in optically isotropic materials is clearly of significant interest in the design of switchable lenses. In this paper, we propose the use of the Dark Conglomerate (DC) phase [12, 13], which occurs in some bent-core liquid crystals, to form variable lenses. Recent observations report a significant polarization-insensitive change in refractive index with respect to an applied field [14], offering a new approach to polarization-independent electro-optic devices. An important advantage of the DC phase is that it requires no alignment agent on the substrate of the device and such simplicity in construction (only a single liquid crystal layer is needed for successful lens operation) is of particular relevance for its potential use in devices. The important

characteristics of the DC phase can be summarized as follows. The DC phase is an optically isotropic liquid crystal phase, with polarizing microscopy revealing a dark texture when analyzing the DC phase using crossed polarizers, with chiral domains of opposite handedness observed when uncrossing the polarizers. The DC phase usually occurs at temperatures directly below the isotropic phase of the material, and is understood to consist of tilted polar smectic layers with a short interlayer correlation length [12].

The DC phase that occurs in the oxadiazole-based achiral bent-core mesogen OC12-Ph-ODBP-Ph-C5 (material designated VBG93) has some unusual properties [15]. The DC phase in this material occurs below the nematic phase between 100 °C and 167 °C and shows unusual behavior in response to an applied electric field. In particular, a large, isotropic variation in refractive index with respect to applied electric field has been reported, which is not observed in other materials [14, 16]; this is the first material discovered with the electro-optic response. Three distinct regimes of the electric-field dependence of the DC phase are observed in VBG93 that are both temperature and frequency dependent. For $T = 162^\circ\text{C}$ and an AC field of frequency of 550 Hz the behavior is: for $8 \text{ V}\mu\text{m}^{-1} < \mathbf{E} < 11 \text{ V}\mu\text{m}^{-1}$ an optically uniform texture is observed under crossed polarizers; for $\mathbf{E} > 14 \text{ V}\mu\text{m}^{-1}$ optically isotropic domains of opposite handedness are observed; and for $\mathbf{E} > 18 \text{ V}\mu\text{m}^{-1}$ an isotropic, achiral texture is induced.

We are primarily concerned with the large change in refractive index which occurs for applied field strengths between $14 \text{ V}\mu\text{m}^{-1} < \mathbf{E} < 18 \text{ V}\mu\text{m}^{-1}$ shown in the shaded region of Fig. 1. A reduction in refractive index of from 1.66 to 1.62 is observed such that the total change in refractive index in this region is ~ 0.04 . The reduction in refractive index of the DC phase is a property that can be used to form variable focus lenses, as described below. While the overall principle of varying the focus *via* a change in refractive index is similar to that used in nematic liquid crystal based lenses, in this case the change in refractive index is electric-field driven rather than voltage driven. This subtle difference allows new modes of operation and additional complexities to be generated in the switchable lenses. In this paper, we describe a computational simulation assessing the use of the DC phase in switchable lenses, using techniques previously used to analyze gradient-index lenses and liquid crystal contact lenses [17, 18]. We demonstrate that the DC phase shows remarkable potential for lens-based applications due to the field-dependent isotropic change in refractive index; the computational assessment considers its use in two different types of lenses. We show that the electric-field driven change in refractive index allows the DC phase to be used in microlenses using a lens shaped liquid crystal layer and in flat GRIN lenses. Interestingly, the variable thickness of the liquid crystal layer in the microlens and the field-dependent behavior of the DC phase allows the design of lenses which can have both a negative and positive focal length, depending upon the amplitude of the applied field.

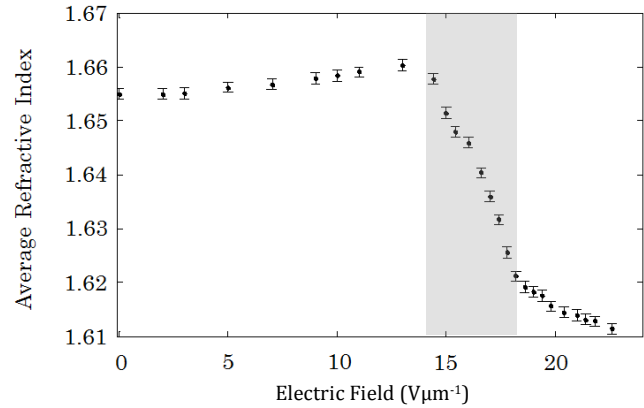


Fig. 1. Refractive index (at 589 nm) as a function of applied field measured through analysis of the reflection spectrum of a thin film of the material [14, 15]. The shaded region is of particular interest ($14 \text{ V}\mu\text{m}^{-1} < \mathbf{E} < 18 \text{ V}\mu\text{m}^{-1}$); a small increase in field produces a refractive index change of 0.04. Measurements are at 162 °C using a 550 Hz AC field.

2. Computational Methods

In order to model the operation of a liquid crystal lens that employs the DC phase of VBG93 successfully, two main parameters need to be calculated; the electric field within the device and a subsequent calculation of the refractive index of the liquid crystal. The electric potential (ϕ) within a liquid crystal device can be calculated by the solution of the differential form of Gauss' Law, $\nabla \cdot \mathbf{D} = 0$, where \mathbf{D} is the electric displacement vector ($\mathbf{D} = \epsilon\mathbf{E}$), as has been shown in detail in a previous publication [17]. By definition of the boundary conditions of the electric potential within a device, this equation can be digitized and solved numerically using MATLAB (R2008, Mathworks, Natick, USA). Mirror boundary conditions are applied in the horizontal direction while in the vertical direction the boundary conditions are fixed. Since the solution for the potential scales with distance, all grid spacing are fixed at unity for ease of computation. Several numerical methods were utilized to model the electric potential within liquid crystal devices, as described in previous work, including red / black ordering to improve convergence times and successive over relaxation (SOR) methods to ensure stable solutions [17, 19]. A multigrid method was used to speed up convergence. The numerical solution was initially solved on a coarse grid, with the simulation grid becoming increasingly finer with each additional iteration, using the information from the previous grid to speed up simulations times by up to a factor of 40. The process of refining, interpolating and solving is repeated until the finest grid required has been achieved. The output of the calculation is a grid of simulation points with a value of electric potential deduced from the initial boundary conditions. After simulation of the electric potential ϕ within the device, the electric field \mathbf{E} can be calculated using $\mathbf{E} = -\nabla\phi$.

From a simulated grid of electric field values, the corresponding refractive index of the simulation points can be approximated by interpolation of the data shown in Fig. 1. Once

refractive index profile within the device has been calculated, the Optical Path Length (OPL) for light travelling through different parts of the device can be calculated and the focal power can be determined *via* ray tracing. We note that the simulation of the flat GRIN lenses described in Section 4 was substantially faster and more effective than the microlenses of Section 3 due to the simpler device geometry of the former.

3. Simulation of a Microlens

The microlens modeled is defined by the geometry of the system shown in Fig. 2. In this arrangement we consider a liquid crystal device consisting of a planar ITO coated glass layer and a convex lens ITO coated glass layer. Note that as the DC phase is used, there is no need to include the alignment layer, which is vital in similar nematic devices. When placed together, the two substrates form a cavity taking the shape of a plano-concave lens which can be filled with a liquid crystal. Key parameters to be calculated include the electric field within the device, the refractive index distribution within the liquid crystal layer and finally a calculation of the wave front to determine the optical properties of the lens.

The optical calculations assume that the lens is thin with the effective focal power, F , given by,

$$F = \frac{1}{f} = (n - 1) \left[\frac{1}{R_1} - \frac{1}{R_2} \right], \quad (1)$$

where f is the focal length of the lens, n is the refractive index, and R_1 and R_2 are the top and bottom radii of curvature respectively of the lens. By careful variation of R_1 and R_2 equal converging and diverging focal power can be induced in the glass convex lens and the liquid crystal layer respectively; such a system is known as *balanced*. Upon application of an electric field across the liquid crystal layer, the optical power in the system changes, resulting in a variable focus. In this example, the optical power of the glass and DC layers were +347 D and -347 D respectively when unpowered, assuming the refractive indices of glass and the DC phase to be $n_{\text{glass}} = 1.5$ and $n_{\text{dc}} = 1.655$ respectively and radii of curvatures $R_1 = 5950 \mu\text{m}$ and $R_2 = -1900 \mu\text{m}$. Upon the application of a sufficiently high field, the refractive index of the DC phase reduces towards $n_{\text{dc}} = 1.61$ (see Fig. 1), which results in an increase in optical power of the LC layer from 0 D to 20 D. The large optical power associated with each of these layers is a consequence of the geometry chosen, in particular due to the microlens system and different optical powers would of course be obtained for larger lenses. In the simulated device we consider a $100 \mu\text{m}$ diameter lens, in which the liquid crystal layer is $5 \mu\text{m}$ thick at the center of the device and increases to $5.65 \mu\text{m}$ at the edge. The dielectric permittivity of the DC phase is taken to be 22, as measured experimentally at 162°C , and the assumption of a constant value for ϵ is the same approximation as has been made in other simulations [17].

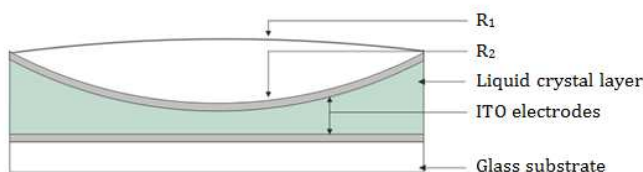


Fig. 2. A diagram of the microlens used for the computational simulations in this work. R_1 and R_2 are $5950 \mu\text{m}$ and $-1900 \mu\text{m}$

respectively, with a lens diameter of $100 \mu\text{m}$. In the off state the optical power of the liquid crystal layer and the glass substrates are opposite and equal, yielding zero optical power. The application of a field induces a field-induced focus *via* the change of the focal power of the liquid crystal layer, resulting in positive optical power from the device.

A simulation grid of 4000 by 228 points was used for calculations of the electric potential within the device, with a grid spacing of $0.025 \mu\text{m}$. A relatively fine grid was required due to the curvature of the simulated electrodes and the requirement to digitize this into boundary conditions. Despite the fine grid employed, some digitization of the solutions is apparent.

The field-dependent properties of the refractive index in the DC phase offer a unique opportunity for switchable microlens designs. Initially the lens is in the off state and, as the overall lens is designed to be balanced, the optical path difference is constant across the device. The application of high voltages ($>120 \text{ V}$) across the device is sufficient to saturate the field-response of the DC phase (the field is in excess of $20 \text{ V}\mu\text{m}^{-1}$) and in this situation the refractive index is uniform in the liquid crystal layer with a refractive index of 1.615. The induced focal power is calculated to be +20 D through an analysis of the emergent wave front, which is in agreement with calculations that use Eqn. 1. An interesting phenomenon occurs upon application of lower voltages, in this case 90 V; a gradient-index lens is induced as a result of the non-uniform electric field in the device and a negative lens is induced, with a diverging optical power of -85 D. At other voltages for this particular system, either parts of the lens remain unswitched (low field regime), or there is mix of gradient index and saturation (higher field regime), resulting in wave fronts that have severe aberrations. Thus there are effectively only two useful field-driven states for this lens geometry. A comparison of the emergent wave fronts across the lens is shown in Fig. 3 for the three values of applied voltage of interest. A calculation of the refractive index profile across the lens with 90 V applied is shown in Fig. 4 to illustrate the induction of the gradient index lens. Clearly, the lens exhibits two modes of operation, a positive lens based upon a uniform bulk change in refractive index at high voltages, and a negative lens based upon a gradient index effect at intermediate voltages.

Aberrations (in this case wavefront deviations from a parabolic phase retardation profile) can be minimized by ensuring that the lens operates in the region between $16 \text{ V}\mu\text{m}^{-1} < E < 18 \text{ V}\mu\text{m}^{-1}$, where the change in refractive index is approximately linear. In order to meet this condition, the maximum change in liquid crystal thickness between the center and the edge of the device is required to be less than $0.65 \mu\text{m}$ when working with a $5 \mu\text{m}$ thick liquid crystal layer in the center of the lens. In order to change the focal power of the negative power state, the central thickness of the lens can be varied to provide more or less phase retardation between the edge of the lens and the center as a result of the non-linear electric field in the device. However, a reduction in the central thickness of the device increases the difference in electric field between the center of the lens and the edge. Hence, designing a lens with a specific diverging GRIN mode of operation requires balancing of the thickness of the liquid crystal layer and the radius of curvature of the top substrate.

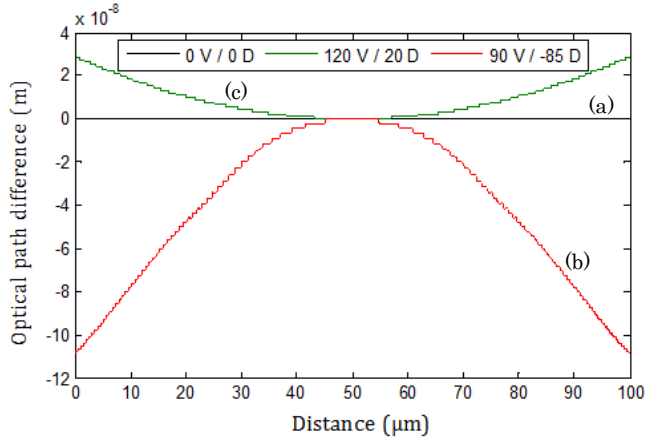


Fig. 3. A computational analysis of the phase retardation of the lens shown in Fig. 2 with operating voltages of (a) 0 V (black), (b) 90 V (red) and (c) 120 V (green). The optical path difference (OPD) is taken with respect to the center of the lens to determine the wave front. A wave front associated with converging optical power (+20 D) is induced by voltages >120 V. A phase retardation profile associated with diverging optical power can be induced via the application of 90 V. Slight digitization of the wave fronts can be seen; as mentioned, this is a result of the simulation resolution.

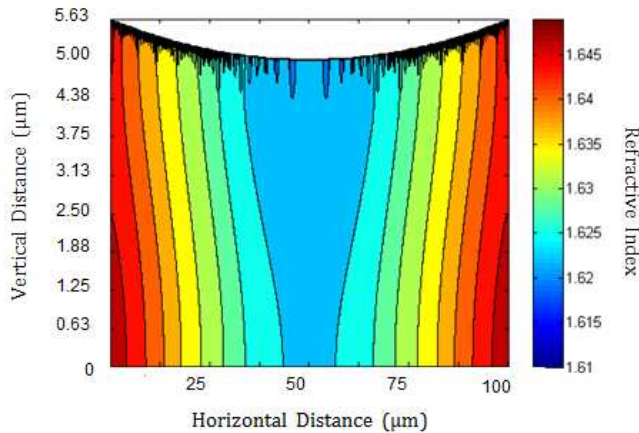


Fig. 4. The calculated refractive index in the liquid crystal layer of the device of Fig. 2 at a wavelength of 589nm and at an operating voltage of 90 V, illustrated using ten discrete color bands. The variation of refractive index represents a gradient-index profile which induces a diverging wavefront, indicated in Fig. 3. The noise at the curved boundary is a consequence of the resolution of the calculation.

4. Simulation of a Flat GRIN Lens

Simulations were also conducted to assess the use of the DC phase in a GRIN lens; with a parabolic voltage distribution used to induce focal power in a flat liquid crystal layer. There are many methods of providing a parabolic voltage across a liquid crystal layer, in this case we consider a device in which an insulating glass layer and two electrodes are used, as shown in Fig. 5. The equation to determine the focal power of a GRIN lens is given by;

$$F = \frac{1}{f} = \frac{2\Delta nk}{(d/2)^2}, \quad (2)$$

where Δn is the maximum change in refractive index between the center and the edge of the lens, k is the thickness of the GRIN medium and d is the diameter of the lens.

In this instance, a 5 μm thick liquid crystal layer is used with a 50 μm thick glass insulation layer, which provides a parabolic voltage distribution across the liquid crystal layer. The wavefront is analyzed to determine the optical power and identify any aberrations in the device.

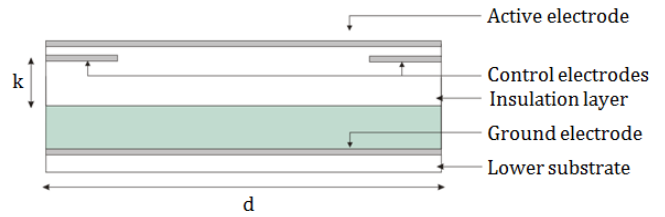


Fig. 5. A diagram of the GRIN lens geometry used for the computation simulations. The optical zone between the two active electrodes is set to 100 μm with a gap of 1 μm between the active and control electrodes.

A simulation grid of 120 by 45 points was used for calculations of the electric potential within the device, with a grid spacing of 1 μm . A comparison of the emergent wave front across the lens for different values of applied voltage is shown in Fig. 6. Focal powers up to +83.5 D could be induced when fields in the region between $16 \text{ V}\mu\text{m}^{-1} < \mathbf{E} < 18 \text{ V}\mu\text{m}^{-1}$ were induced within the liquid crystal layer.

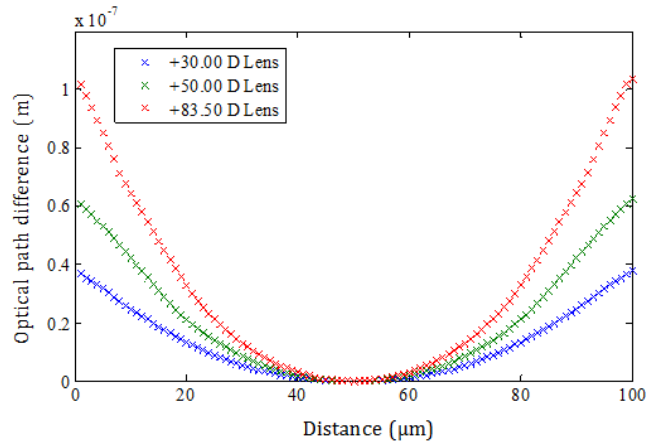


Fig. 6. Emergent wave fronts for the GRIN lens shown schematically in Fig. 5 for different values of induced focal power. Lenses corresponding to +30 D (blue, lower data set), +50 D (green, middle data set) and +83.5 D (red, top data set) show minimal aberrations, with the wave front corresponding to a parabolic phase retardation.

The maximum focal power of +83.5 D was induced with a surface voltage on the liquid crystal layer that varied from 80 V in the center to 90 V at the edges. Such a case corresponds to the electric field within liquid crystal layer taking values in the linear regime, i.e., in the range $16 \text{ V}\mu\text{m}^{-1} < \mathbf{E} < 18 \text{ V}\mu\text{m}^{-1}$. In terms of driving such a device, such surface voltages correspond to an active voltage of 2390 V and a control voltage of 3190 V applied

above the glass insulation layer. Calculated focal powers of +30 D and +50 D are induced with the application of an active voltage of 2420 V and control voltages of 2690 V and 2900 V respectively. The operating voltages are very high, and so the insulation layer must have a sufficiently high dielectric strength to prevent dielectric breakdown. Three wavefronts corresponding to optical powers of +83.5 D, +50 D and +30 D are shown in Fig. 6, with similar optical quality and a parabolic wave front in each of these states. In addition, the refractive index profile for a +83.5 D lens is shown in Fig. 7 to illustrate the gradient index profile of the liquid crystal in this device. Again, the relatively large optical powers quoted for this system are associated with the lens geometry chosen.

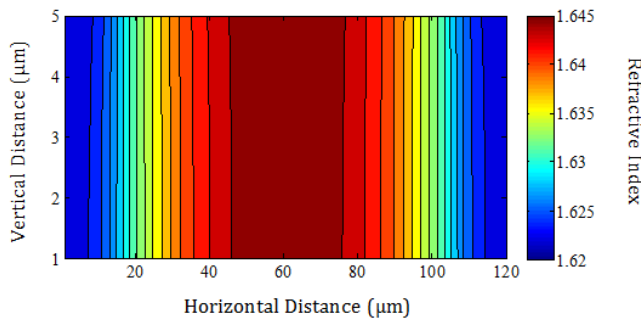


Fig. 7. Calculation of the refractive index profile (at a wavelength of 589nm) in a 5 μm thick liquid crystal layer of a GRIN lens, with a resultant optical power of +83.5 D. N discrete color bands are used in the plot. The DC layer is subject to parabolic electric field strengths between 16 and 18 $\text{V}\mu\text{m}^{-1}$ in the center and at the peripheries of the device respectively. Such a situation corresponds to minimal aberrations as shown in Fig. 8. The electric field distribution results in a parabolic refractive index profile throughout the DC layer.

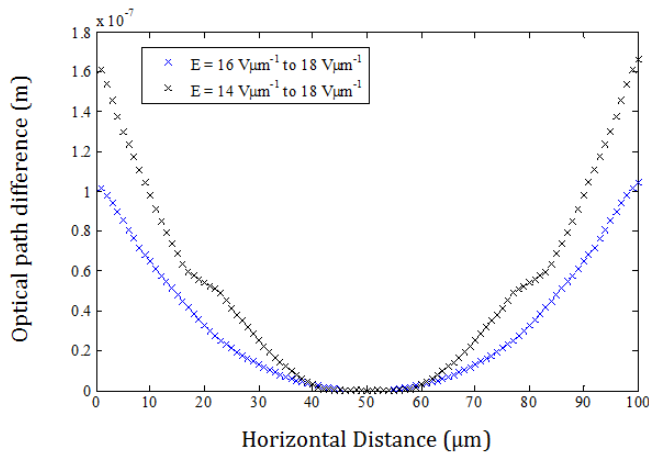


Fig. 8. A comparison of the phase retardation profiles produced when the liquid crystal experiences a parabolic electric field difference of 16 to 18 $\text{V}\mu\text{m}^{-1}$ between the centre and the edge of the device (blue points, lower data set), and 14 to 18 $\text{V}\mu\text{m}^{-1}$ (black points, upper data set). The phase retardation profile when working in the latter region is larger in magnitude but with aberrations caused by the non-linear nature of the refractive index change with respect to electric field (see Fig. 1).

It was found that aberrations were minimized when working in the region of $16 \text{ V}\mu\text{m}^{-1} < \mathbf{E} < 18 \text{ V}\mu\text{m}^{-1}$ due to the linear nature of the change in refractive index with respect to

applied field, with a comparison of the emergent wave front when working with the regions of $16 \text{ V}\mu\text{m}^{-1} < \mathbf{E} < 18 \text{ V}\mu\text{m}^{-1}$ and $14 \text{ V}\mu\text{m}^{-1} < \mathbf{E} < 18 \text{ V}\mu\text{m}^{-1}$ shown in Fig. 8. This restriction in the electric field limits the focal power of the device, with an operational refractive index change of ~ 0.021 rather than 0.04, but offers excellent quality of switchable lenses.

6. Discussion and Conclusions

This paper has assessed the potential of the DC phase for use in two different 100 μm diameter lenses, utilizing both conventional optics and GRIN optics as shown in Fig. 2 and Fig. 5 respectively. Due to the electric field driven nature of the change in refractive index, the DC phase exhibits the ability to form microlenses which can operate conventionally to give positive optical power *via* a bulk change in refractive index and which can unusually also provide negative optical power *via* gradient index optics. In addition, flat GRIN liquid crystal devices can employ the change in refractive index of the DC phase to form optical devices similar to those that make use of nematic liquid crystals but with the significant advantage of being polarization independent. This work illustrates that the DC phase has excellent potential for the development of a new class of polarization-independent switchable liquid crystal lenses.

One of the fundamental conclusions gained from this work is that the field-dependence of the refractive index in the DC phase leads to some unexpected lens behavior. Although the maximum change in refractive index for the example considered occurs for $14 \text{ V}\mu\text{m}^{-1} < \mathbf{E} < 18 \text{ V}\mu\text{m}^{-1}$, the optimum operational range for lens use appears to be $16 \text{ V}\mu\text{m}^{-1} < \mathbf{E} < 18 \text{ V}\mu\text{m}^{-1}$ due to the approximately linear relationship between refractive index and electric field in this region. Although the maximum operational power of GRIN-based modes is reduced by limiting the field to the linear regime, the wave front aberrations are reduced and excellent optical quality of the lenses is predicted.

When comparing the two types of devices that have been simulated (microlenses, Fig. 2 and flat GRIN lenses, Fig. 5), the main difference is in the variability of focal power that can be achieved. In the case of the flat GRIN structure, the focal power can be varied continuously between 0 D and +83.5 D, while the microlens device chosen as an exemplar is restricted to three optical states, 0 D, -85 D and +20 D. In the flat GRIN lens, the operating voltages are high (~ 1 kV) due to the inclusion of the insulation medium, resulting in far higher input voltages than are desirable in a device and than are required to drive the microlens structure (typically ~ 100 V). However, there are other methods of providing the parabolic voltage distribution required in the GRIN lens which can reduce the operating voltages substantially, such as the use of a high ϵ dielectric layer or the use of a resistive layer for modal control of the lens [6, 11]. In both forms of liquid crystal lenses described in this paper, the operating voltages can be reduced by reducing the thickness of the liquid crystal layer. When working with the microlens, the curvature of the device would require modification in a thinner device in order to provide a high quality GRIN mode of operation *via* non-uniform electric field strength. In either of the lenses described, reducing the thickness of the liquid crystal layer will result in decreased optical power when working with GRIN optics. The use of the DC phase in other lens geometries, such as a microlens with plano-convex DC layer, could be considered which would result in additional modes of operation.

In terms of comparison with existing technology, the major advantage that DC phase lenses would have over nematic devices is that the change in refractive index is polarization insensitive, which allows a single liquid crystal layer to be used. In addition, the DC phase requires no alignment agent, which simplifies construction procedures. In comparison with lenses that have been designed using the Kerr effect in blue phase liquid crystals [11], the change in refractive index in the DC phase is approximately linear with field and has a standard dispersion relationship, both of which are significant advantages when considering optical use. In contrast, the Kerr effect is proportional to the square of the field, is strongly wavelength dependent and, importantly, the Kerr effect induces birefringence rather than the isotropic change in refractive index induced in the DC phase. The magnitude of the field-dependent change in refractive index in the DC phase is comparable to that induced by the Kerr effect in blue phase liquid crystals.

Research into the DC phase is in its infancy but the unique electro-optic properties show real promise for devices. So far, the response time of the electro-optic effect in the DC phase has not been investigated and this of course will be critical to any final applications of the phenomenon. Further, the high temperature at which the electro-optic measurements were made in this first material is also unacceptable for device applications. New developments, moving towards lower temperature DC phases with lower operating voltages will allow practical applications. The natural next stage of development is the construction of DC based lenses in order to confirm their proposed use in optical devices and to identify optimum construction techniques.

Acknowledgments

VBG93 was developed by J W Goodby and V Görtz under various collaborative EPSRC projects (EP/G023093/1 and EP/D055261/1). This work has been funded by University of Manchester Intellectual Property (UMIP) and MTI Ventures. MN would like to acknowledge the Royal Commission for the Exhibition of 1851 for a fellowship. JCJ wishes to thank the EPSRC for support through an Advanced Manufacturing Fellowship (EP/L015188/1). The authors thank Paul Brimicombe for helping to develop the simulation software used in this work.

References

1. G. D. Love, "Handbook of Liquid Crystals," in *Adaptive Optics and Lenses*, J. W. Goodby, P. J. Collings, T. Kato, C. Tschierske, H. F. Gleeson, and P. Raynes, eds. (Wiley-VCH, 2014), p. 945.
2. S. Sato, "Liquid-crystal lens-cells with variable focal length," *Jpn. J. Appl. Phys.* **18**, 1679-1684 (1979).
3. S. Sato, A. Sugiyama, and R. Sato, "Variable-Focus Liquid-Crystal Fresnel Lens," *Jpn. J. Appl. Phys. Part 2-Letters* **24**, L626-L628 (1985).
4. H. E. Milton, P. B. Morgan, J. H. Clamp, and H. F. Gleeson, "Electronic liquid crystal contact lenses for the correction of presbyopia," *Opt. Express* **22**, 8035-8040 (2014).
5. M. Ye, B. Wang, and S. Sato, "Liquid-crystal lens with a focal length that is variable in a wide range," *Appl. Opt.* **43**, 6407-6412 (2004).
6. A. F. Naumov, M. Y. Loktev, I. R. Guralnik, and G. Vdovin, "Liquid-crystal adaptive lenses with modal control," *Opt. Lett.* **23**, 992-994 (1998).
7. B. Wang, M. Ye, M. Honma, T. Nose, and S. Sato, "Liquid crystal lens with spherical electrode," *Jpn. J. Appl. Phys. Part 2-Letters* **41**, L1232-L1233 (2002).
8. G. Li, D. L. Mathine, P. Valley, P. Åyräs, J. N. Haddock, M. S. Giridhar, G. Williby, J. Schwiegerling, G. R. Meredith, B. Kippelen, S. Honkanen, and N. Peyghambarian, "Switchable electro-optic diffractive lens with high efficiency for ophthalmic applications," *Proceedings of the National Academy of Sciences* **103**, 6100-6104 (2006).
9. C.-H. Lin, H.-Y. Huang, and J.-Y. Wang, "Polarization-Independent Liquid-Crystal Fresnel Lenses Based on Surface-Mode Switching of 90 Twisted-Nematic Liquid Crystals," *Photonics Technology Letters, IEEE* **22**, 137-139 (2010).
10. Y. Mao, W. Bin, and S. Sato, "Polarization-independent liquid crystal lens with four liquid crystal layers," *Photonics Technology Letters, IEEE* **18**, 505-507 (2006).
11. Y. Li, Y. Liu, Q. Li, and S.-T. Wu, "Polarization independent blue-phase liquid crystal cylindrical lens with a resistive film," *Appl. Opt.* **51**, 2568-2572 (2012).
12. L. E. Hough, M. Spanuth, M. Nakata, D. A. Coleman, C. D. Jones, G. Dantlgraber, C. Tschierske, J. Watanabe, E. Korblova, D. M. Walba, J. E. MacLennan, M. A. Glaser, and N. A. Clark, "Chiral isotropic liquids from achiral molecules," *Science* **325**, 452-456 (2009).
13. J. Thisayukta, Y. Nakayama, S. Kawauchi, H. Takezoe, and J. Watanabe, "Distinct formation of a chiral smectic phase in achiral banana-shaped molecules with a central core based on a 2,7-Dihydroxynaphthalene unit," *Journal of the American Chemical Society* **122**, 7441-7448 (2000).
14. M. Nagaraj, V. Görtz, J. W. Goodby, and H. F. Gleeson, "Electrically tunable refractive index in the dark conglomerate phase of a bent-core liquid crystal," *Appl. Phys. Lett.* **104**, 021903 (2014).
15. V. Görtz, C. Southern, N. W. Roberts, H. F. Gleeson, and J. W. Goodby, "Unusual properties of a bent-core liquid-crystalline fluid," *Soft Matter* **5**, 463-471 (2009).
16. M. Nagaraj, K. Usami, Z. Zhang, V. Görtz, J. W. Goodby, and H. F. Gleeson, "Unusual electric-field-induced transformations in the dark conglomerate phase of a bent-core liquid crystal," *Liquid crystals* **41**, 800-811 (2014).
17. H. Milton, P. Brimicombe, P. Morgan, H. Gleeson, and J. Clamp, "Optimization of refractive liquid crystal lenses using an efficient multigrid simulation," *Opt. Express* **20**, 11159-11165 (2012).
18. H. Milton, H. Gleeson, P. Morgan, J. W. Goodby, S. Cowling, and J. Clamp, "Switchable liquid crystal contact lenses: dynamic vision for the ageing eye," *Proceedings of the SPIE* **9004** (2014).
19. U. Trottenberg, *Multigrid* (Academic Press, 2001).